Pergamon

Cement and Concrete Research, Vol. 27, No. 9, pp. 1319–1331, 1997

0008-8846/97 $17.00 + 00

PII S0008-8846(97)00137-3

EFFECTS OF DRYING AND FREEZE/THAW CYCLING PROBED BY ^{1}H-NMR

Hans Chr. Gran* and Eddy Walther Hansen**
*Norwegian Building Research Institute, P.O. Box 123, Blindern, N-0314 Oslo, Norway/ University of Oslo, Dept. of Chemistry, P.O. Box 1033, Blindern, N-0315 Oslo, Norway
**SINTEF, P.O. Box 124, Blindern, N-314 Oslo, Norway

(Refereed)
(Received November 27, 1996; in final form July 28, 1997)

ABSTRACT

^{1}H-NMR spin lattice relaxation times, T_1, of water occupying the pore system in white hydrated cement pastes have been measured to probe the effect of drying and freeze/thaw cycling on the pore structure. Surface to volume ratios and specific surface areas are derived from these NMR measurements. Specific surface areas vary from 132 m^2/g for w/c = 0.30 to 242 m^2/g for w/c = 0.70. A significant increase in T_1 is observed after drying tests performed at 105°C on pastes with w/c-ratios 0.30, 0.40, 0.60 and 0.70 corresponding to a reduction in specific surface area of 33.0, 25.0, 7.1 and 6.5%, respectively. Line width measurements showed significant reduction only for the w/c = 0.30 sample. The results are in agreement with earlier work and imply that the pore structures related to micro and meso pores are more vulnerable to drying than the coarser pore structures. Freeze/thaw cycling show no significant changes in T_1 after 25 cycles although all samples except one are fragmented by frost action. However, a small increase is observed after 175 cycles for samples with the lower w/c-ratios. © *1997 Elsevier Science Ltd*

Introduction

The pore size distribution in hydrated cement pastes covers a wide range of different pore radii from a few Ångstroms to several hundred microns. Powers and Brownyard (1) divided the pore system into two categories. 1. Gel pores which are created during hydration as the different crystals and gel products develop. They are intrinsic to the hydrated cement paste and consist of micro (pore radius, R ≤ 10 Å) and mesopores (10 Å < R < 100 Å). 2. Capillary pores which originates from excess water not taking direct part in the hydration, i.e. only present at water/cement-ratios (w/c) above about 0.40. Although later work (2) based on mercury intrusion porosimetry (MIP), gas adsorbtion and freeze calorimetry indicate that the pore size distribution is continuous, the model of Powers and Brownyard still gives a useful description. In a hydrated cement paste, the gel pores are filled by surface adsorbed water whereas the capillary pores are filled by capillary condensed water.

It is well known that the pore system of virgin hydrated cement paste is significantly and irreversibly affected by drying. Powers et al. (3) observed a large increase in permeability to water as a result of drying and resaturation. Parrot et al. (4) found large losses of inner surface

area after drying. Using freeze calorimetry, Bager and Sellevold (5,6) concluded that drying and resaturation resulted in a coarser pore system. Lawrence et al. (7) described this as an irreversible partial collapse of the pore structure. Winslow and Diamond (8) found, using small angle X-ray scattering, that the inner surface area was reduced from 700–800 m^2/g to 200 m^2/g in cement pastes of w/c 0.40–0.60. Jacobsen and Sellevold (9) reported larger effects of drying at higher w/c-ratios.

The existence of a pore system which may be filled with water makes the cement paste susceptible to freezing and thawing. Powers presented an hypotheses (10) for freezing mechanisms which cause frost damage in hydrated cement pastes and concrete. He assumed that ice formation starts from the surface and causes an hydraulic pressure buildup in the unfrozen water due to the 9% volume increase of water upon freezing, which in turn damages the cement paste. In addition to the hydraulic pressure model of Powers, Collins (11) explained the frost action by the growth of ice lenses owing to migration of water from capillaries where the freezing point is depressed, whereas Powers and Helmuth (12) placed the responsibility on localized osmotic pressure. The mechanism of frost deterioration is still not fully understood. Few workers have studied the effects of freezing and thawing on the pore structure. MIP investigations performed by Bager and Sellevold (6) showed an increase in the volume of both smaller and coarser pores. Kayali et al. (13) found a coarsening of the pore structure. Nakamura (14) found an increase of the amount of coarser pores and a reduction of the amount of finer pores around 100–500 Å. Kukko (15) measured a shift in size distribution to smaller pores.

During the last two–three decades nuclear magnetic resonance (NMR) spectroscopy has developed into an important tool for characterization of porous materials (16). The technique has become a valuable supplement to other principal techniques such as low temperature calorimetry, MIP, gas adsorption/desorption, low angle X-ray scattering and optical/electron microscopy. In contrast to most other techniques, NMR is non destructive and does not require any kind of drying or vacuum treatment before testing which may cause artificial changes to the structure of some materials. Pore size distribution derived from NMR is based on a well established correlation between the spin lattice relaxation time T_1 of liquids confined in porous materials and the surface to volume ratio of the pore system (17). Some work has also been done on liquids occupying the pore system of hydrated cement pastes. Blinc et al. (18) and Bhattacharja et al. (19) studied the hydration of cement pastes by measuring T_1 and T_2 respectively. Gran and Hansen (20) looked at the exchange process between water and ethanol in the pore system of cement pastes and correlated T_1 with pore radius, R, obtained from mercury intrusion porosimetry experiments.

The purpose of this work has been to apply the experiences from work on T_1 and pore radius, R (17.21,22) to see how changes in the pore structure introduced by drying at 105°C affects T_1 and NMR line width measured in water occupying the pore system in hydrated cement pastes. Based on this experience, similar measurements have been performed on cement pastes exposed to freeze/thaw cycling where the impact on the pore structure is less known.

Experimental

Specimens. Samples of hydrated cement paste (HCP) with four different water to cement (w/c) ratios were used in the experiments. The mix ratios were w/c = 0.30 (sample S03), 0.40

TABLE 1
Oxide composition of white Portland cement given as percent by weight of oxide compared to total amount of cement

Oxide	% by weight
SiO_2	24.0
CaO	71.0
Al_2O_3	2.10
Fe_2O_3	0.31
MnO	0.012
MgO	0.55
K_2O	0.04
Na_2O	0.14
SO_3	1.23
Loss on ignition	0.67

(Samples S04, F04a, F04b, F04c), 0.60 (Samples S06, F06a, F06b, S06c) and 0.70 (Samples S07a, S07b). Samples denoted by the letter F were used for freezing and thawing experiments whereas samples denoted by S were used for drying and resaturation tests. All pastes were made from a Danish Super White Portland Cement certified as a British Standards Institution class 62.5N cement, with a Bogue composition of 65.8% tricalcium silicate (C_3S), 21.0% dicalcium silicate (C_2S), 4.18% tricalcium aluminate (C_3A), 0.96% tetracalcium alumina ferrite (C_4AF) and 2.32% calcium oxide (C) and a Blaine surface of 4000 cm^2/g. The reason for using a white cement was its low content of paramagnetic constituents as Fe_2O_3 and Mn_2O_3 which may contribute to NMR relaxation. The composition of the cement was determined by X-ray fluorescence spectroscopy and atomic absorption spectrometry, Table 1. The pastes were mixed under slight vacuum to avoid entrapped forms with diameter 20 mm and length of 120 mm. The total weight of the mixtures were checked before and after mixing to detect any loss of water resulting from the vacuum treatment. The pastes were slowly rotated during the first 20 hours of hardening to avoid separation between water and cement. After demolding, the H_2O-paste was stored in water at room temperature. The samples were 8 months old at the time of testing. The samples were cut from the interior of the molded cylinders to avoid possible inhomogeneities in the paste caused by the proximity to the form walls. Samples F04a,b,c and F06a,b,c were transferred to polyethylene containers for freeze thaw cycling. Samples S03 and S07 were used to see the effect of drying/pore structure modification on spin lattice relaxation time.

NMR. The spin lattice relaxation times, T_1, were measured on a Bruker CXP 200 NMR instrument, operating at 200 MHz proton resonance frequency. All measurements were performed using a simple inversion recovery ($180° - \tau - 90°$) pulse sequence with τ being the time variable. The applied 90° pulse was 6 μs with a repetition time of 300 ms between pulses. The bandwidth was set to 100 kHz using an acquisition time of 0.082 s. A total of 16 transients were accumulated for each τ-value. The samples of hydrated cement paste were cut and ground to a diameter of 3.5 mm and a length of 10 mm and stored in small amounts of

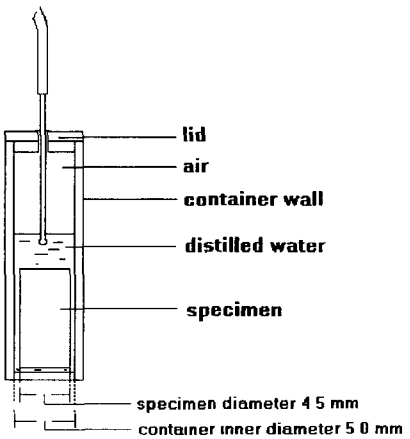

FIG. 1.
The illustration shows specimen container with specimen and thermocouple as used during the freeze thaw cycling.

distilled water until testing. Immediately before testing, the samples were transferred to NMR tubes with 4 mm inner diameter (wiping away water on the external surfaces of the sample with an absorbent tissue). Each tube was finally sealed with a plastic cap covered with epoxy to prevent water vapor escaping from the sample. The sample weight was checked immediately before and after the experiment.

The spin lattice relaxation times were determined from the observed magnetization decay curves by an exponential least squares fit to a generalized stretch exponential function of the form

$$M = \sum_{i=1}^{N} M_{0i}[1 - \alpha \exp(-\tau/T_{1i})^{\beta}] \quad (1)$$

where M_{0i} represents the equilibrium magnetization of component i, α is an adjustable parameter which takes into account inhomogeneities in the radio frequency (RF) pulse and equals 2 under ideal homogeneous pulse conditions. The parameter β has been introduced to take account of a possible distribution in relaxation times (23). For $\beta \neq 1$, the magnetization will deviate from a purely exponential decay which signifies a distribution of relaxation times. Eq 1 will thus improve the fit to the observed magnetization decay curve if a distribution of relaxation times is expected without, however, detailing the actual shape of the T_1 distribution. Eq 1 simply represents a convenient way of extracting a single "average" spin-lattice relaxation time if a distribution of relaxation times exists. Moreover, NMR line widths presented in this work are defined as the width at half peak height of the resonance peak.

Freeze/Thaw Cycling. All cement paste specimens were exposed to rapid freeze/thaw cycles in water. The specimens were surrounded by distilled water in polyethylene containers with inner diameter 5.0 mm and inner length of 30 mm. The containers were left in upright position during the freeze/thaw cycles. A thermocouple was passed through a hole drilled in the lid at the top of the container. See Fig. 1. In addition to the thermocouple in the sample

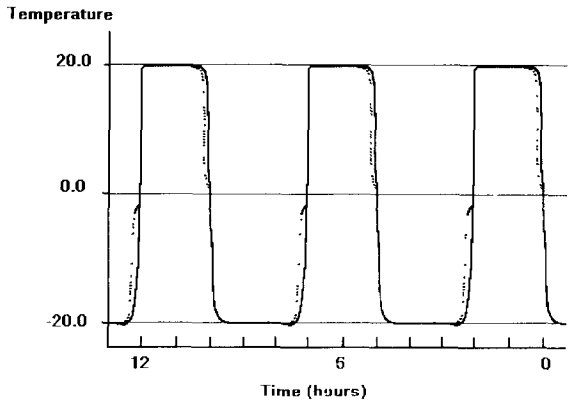

FIG. 2.
Shape of freeze/thaw cycles used in the experiments. Solid line shows air temperature and dotted line shows the sample temperature.

containers, one thermocouple was situated in the air to measure the deviation from the preset cycle. As the samples and containers were small, no notable deviation could be registered.

An air cooled freeze/thaw cabinet manufactured by Brabender Realtest GmbH KSW 512/30 E was used for the freeze/thaw experiments. The cabinet was set to produce 5 freeze/thaw cycles per day which is within the ASTM C666 standard. The temperature range, however, was set to between −20.0°C and 20.0°C, producing a cooling rate registered within the sample container of approximately 2°C per minute. The shape of the cycles is illustrated in Figure 2. All samples were run simultaneously in the freeze/thaw cabinet. NMR spin lattice relaxation times and line widths were measured at 0, 5, 25 and 175 cycles.

Before NMR measurements, the specimens were removed from the containers and wiped dry (saturated surface dry (SSD) condition) with an absorbent tissue and transferred to NMR tubes. As the freeze/thaw cycles went along, some of the specimens suffered from frost damage and separated into smaller pieces. To remove water on external surfaces, the fragments were left for a few minutes on an absorbent paper before transfer to the NMR tubes. After the NMR measurements, the specimens were returned to the freeze/thaw containers and new distilled water added. The freeze/thaw cycling was continued by placing the containers in the cabinet as it ran through a temperature maximum (20.0°C).

Drying at 105°C. To see the effect of drying, T_1 and NMR line widths were measured for specimens S03, S04, S06, S07a and S07b in virgin (never dried) condition and in water-resaturated condition after drying until constant weight at 105°C. Measured weight loss was S03: 13.5%, S04: 18.4%, S06: 27.7% and S07a,b: 32.4%. Resaturation was done by first placing the samples in 100% relative humidity for 24 hours to ensure good adsorption of water in the finer pore structure. Maintaining 100% relative humidity, the samples were thereafter placed with one end in distilled water for capillary suction for another 24 hours before submersion in water. None of the samples regained the original weight. The amount of resaturation in percent, compared to the weight loss caused by drying was measured to: 94.3% (S03), 97.6% (S04), 99.0% (S06), 98.8% (S07a) and 99.4% (S07b).

Results and Discussion

The NMR spin lattice relaxation rate, T_1, and NMR line width measured in liquids occupying a pore structure are significantly influenced by changes in the pore system parameters. Several workers (17,21,24,25) have correlated the measured T_1 or more correctly the relaxation rate ($1/T_1$) to the ratio between inner surface area and the volume of the pore system (S/V). In particular Blinc and coworkers (26) and Letellier and coworkers (27) measured the development of specific surface areas in hydrated cement pastes as a function of hydration time. In general, the observed relaxation rate of a fluid confined in a porous material is considered to consist of two components, the bulk relaxation rate $1/T_{1,B}$ and the relaxation rate experienced by water molecules near the inner surfaces $1/T_{1,S}$. This correlation is described by (17):

$$\frac{1}{T_{1,av}} = \frac{1}{T_{1,B}} + \frac{S}{V}\frac{\lambda}{T_{1,S}} \tag{2}$$

where λ is the thickness of the surface layer and is based on the two fraction fast exchange model of Zimmermann and Brittin (28). Equation 2 is valid under the assumption of fast exchange (on an NMR time scale) between fluid in the interior part of the pore and fluid situated at the surface of the pore. Fast exchange has been observed in studies on hydrating cement pastes (19). The $T_{1,B}$ is normally in the order of one second, whereas the $T_{1,S}$ is in the order of 1–10 ms or even shorter. This is characteristic of molecules experiencing restricted movement where the average time between collisions for translational motion, the correlation time, is shortened. According to the BBP-theory (29), the relaxation rate ($1/T_1$) of molecular (nuclear) motion in the liquid state is proportional to the inverse correlation time.

In cement of w/c = 0.40, S is typically 200 m^2/g and V about 0.2 cm^3/g. The smallest possible thickness of the surface layer corresponds to the size of the water molecule which is approximately 3 Å (19), making the last term in equation 2 of the order of 10^3 to 10^4 larger than the first term. If λ and $T_{1,S}$ are assumed to be the same for the different cement pastes, equation 2 can be simplified to give

$$\frac{1}{T_{1,av}} = \rho\frac{S}{V} \tag{3}$$

where ρ is a constant ($\lambda/T_{1,S}$). The constant ρ is the surface interaction parameter which was described by D'Orazio et al. (17). From equation 3, it is possible to make a relative comparison of the S/V-ratio of different cement pastes from T_1-measurements, although the value of ρ is not known.

From comparison of NMR T_1 measurements and mercury intrusion porosimetry, the relation between $1/T_{1,av}$ and $S\lambda/V$ was found (21) as shown in equation 4,

$$\frac{1}{T_{1,av}} \approx 2.280\cdot 10^3\frac{S\lambda}{V} \tag{4}$$

Assuming bulk density of the pore water (20), V can be found by gravimetric determination of the evaporable water content by drying of cement pastes at 105°C. Using a surface layer thickness $\lambda \cong 3.5$ Å as determined in the literature (21,22) equation 4 can be used to determine the internal specific surface area. It should be pointed out that there is some debate

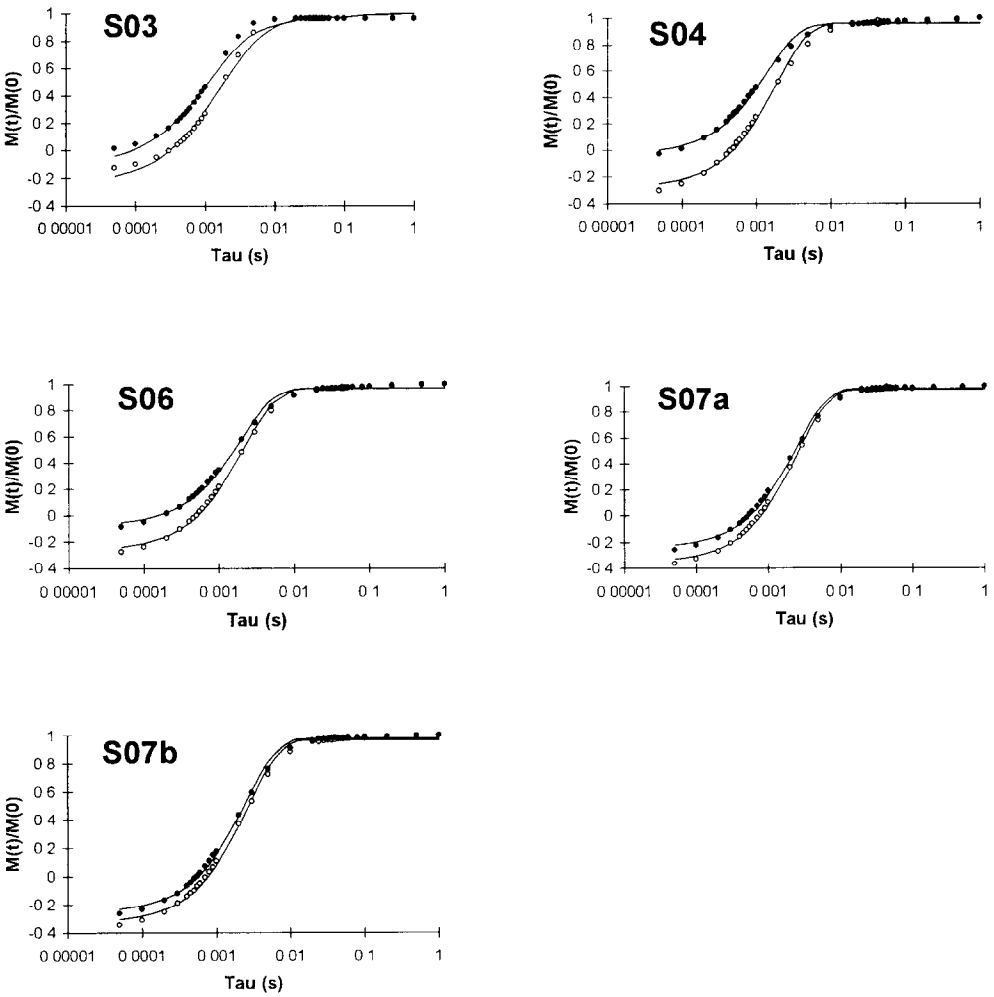

FIG. 3.

Magnetization decay curves measured in virgin (●) samples and after drying at 105°C to constant weight and resaturation with distilled water (○). Solid curves represent least squares fit to the experimental data using a single stretched exponential function, equation 1 (i = 1).

about the value of the surface layer thickness. However, this does not modify the conclusions of this paper since the absolute values of the S/V-ratios are not important in order to see effects of exposure to freezing/thawing and drying. The volumes (V) determined for w/c = 0.30, 0.40, 0.60 and 0.70 in percent of total sample weight where 13, 18, 20 and 43 respectively.

Effect of Drying at 105°C. Figure 3 shows the magnetization decay curves for sample S03, S04, S06 and sample S07a,b (both as virgin and as dried/resaturated). The decay curves indicate significant differences between virgin and dried condition for all samples. Solid curves represent least squares fit of equation 1 to the observed data with i = 1.

TABLE 2

Spin lattice relaxation time, $T_{1,av}$, specific surface area (S: equation 4) and line width (Δ) in virgin hydrated cement pastes S03, S04, S06, S07a and S07b before and after drying at 105°C and resaturation with distilled water. T_1 is calculated by a non linear least squares fit to the magnetization decay curve using eq 1 with i = 1. Uncertainties are given as 90% confidence intervals

Sample	$T_{1,av}$ (ms) virgin	$T_{1,av}$ (ms) dried, resat	S (m^2/g), virgin	S (m^2/g), dried, resat.	δ (kHz) virgin	δ (kHz) dried, resat.
S03	1.35 ± 0.09	2.01 ± 0.08	145 ± 9.0	97.3 ± 3.7	3.3	2.6
S04	1.38 ± 0.06	1.84 ± 0.06	205 ± 8.5	144 ± 4.3	2.7	2.3
S06	1.95 ± 0.08	2.10 ± 0.06	246 ± 9.7	229 ± 6.4	1.5	1.8
S07a	2.45 ± 0.05	2.52 ± 0.06	245 ± 4.9	238 ± 5.6	1.2	1.5
S07b	2.44 ± 0.07	2.61 ± 0.08	246 ± 6.9	230 ± 6.9	1.1	1.3

The numerical values of the model fits are summarized in Table 2, and signify a general increase in $T_{1,av}$ after drying for all samples except sample S07a. The lack of a significant difference in $T_{1,av}$ before and after drying of this sample might be that the inherent experimental sensitivity-limit of the NMR technique is reached. However, as can be seen from Figure 3, the magnetization decay curves between the virgin and the dried sample seem to be visually different, suggesting that the simplified model used in extracting T_1 might be too rough and approximative.

Using equation 4 we have calculated the specific surface area of all samples before and after drying. The results are summarized in Table 2 and show that the w/c-ratio varies from 132 m^2/g in virgin cement paste with w/c = 0.30 to about 240 m^2/g in virgin cement paste with w/c = 0.60 and 0.70. The comparatively low surface area in S03 is consistent with the fact that only a fraction of the cement has reacted due to spatial restrictions and thus lack of water. Within a 90% confidence interval the surface areas are shown to decrease as a result of drying and resaturation with 33% (S03), 30% (S04), 6.9% (S06) and 6.5% (S07b), respectively. Sample S07a shows no significant reductions in specific surface area. These results imply that an opening of the pore structure takes place during drying which is in agreement with earlier work (3,4,6). The finer pore structure in S03 and S04, which mainly is dominated by micro and meso pores, therefore seems to be more vulnerable to drying than the pore structure in S06, S07a and S07b, which also contains a considerable amount of coarser capillary pores. This is in contrast to low temperature calorimetry measurements done by Sellevold and Bager (6) which show large effects after drying for larger pores (R ≅ 60 Å) and little effect of drying for smaller pores (R ≅ 20 Å). It may be explained as low temperature calorimetry is more suited for studies of pores with larger pore radii. Also, the observed line width of the ^1H NMR resonance peaks of the pore confined water of the samples before and after drying are tabulated in Table 2. The estimated uncertainty in NMR line width measurements is approximately ±10% (90% confidence interval). Within this confidence interval the only significant change observed in line width during drying and resaturation was seen in sample S03 which changed from 3.3 kHz to 2.6 kHz. NMR line width thus seems to be less sensitive to changes in the pore system compared to T_1. The line width observed in S03 changes by 21% which is only two thirds the change observed for T_1.

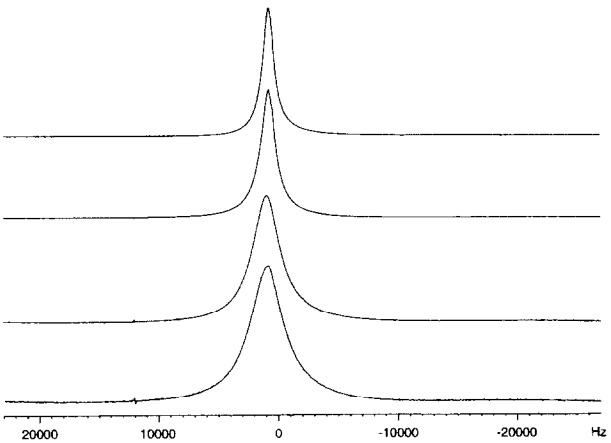

FIG. 4.

^{1}H-NMR spectra of pore water in samples (bottom to top) S03, S04, S06 and S07a. The influence of the w/c-ratio on the line width is evident.

One probable reason for this is that different mechanisms govern the two parameters. This together with larger uncertainty makes the line width parameter less suitable for studying the drying process or changes in the pore structure in general. An example of spectra taken before drying is shown for samples S03, S04, S06 and S07a in Figure 4. A dependence of the line width on the w/c-ratio is evident (from 1.1 kHz for w/c = 0.70 to 3.3 kHz for w/c = 0.30).

The single stretch exponential model (equation 1) used to fit the relaxation curves in Figure 3 revealed β values in the range 0.65–0.83, suggesting a distribution of relaxation times to exist. We have thus fitted the magnetization relaxation curves to a sum of two single exponential functions (eq 1 with i = 2 and β = 1)—in accordance with previous reports (21)—in order to gain more insight into the mechanisms related to the drying process. An example of the improvement obtained in fitting a double exponential function, compared to a single stretched exponential function, to the observed relaxation curves of sample S04 is illustrated in Figure 5.

A description of the water confined in the pore systems by two exponential functions, suggests the existence of two independent and poorly communicating pore systems within the cement paste. Each of these systems is then described by a mean T_1 as presented in eq 2. This does not mean that the two pore systems are isolated from each other, but simply that the exchange of water between them is slow on the NMR time scale. This might for instance originate from narrow pore coupling between the two pore systems causing a diffusion limited exchange of water between them. However, each of the two pore systems might be composed of more than one "pore" size, with an exchange of water between these pores which is fast on the NMR time scale. The spin-lattice relaxation times (double exponential fit) and corresponding specific surface areas (equation 4) of each component of samples S03–S07 are shown in Table 3. Since $M_{0,i}$ in equation 1 is directly proportional to the amount of water contributing to the spin-lattice relaxation time ($T_{1,i}$) in the i'th system, we have tabulated these parameters as relative volumes (V) in Table 3. As can be seen, all samples are characterized by one smaller and one larger T_1. The smaller T_1 represents a system consisting of a larger portion of finer pores than the one with the longer T_1.

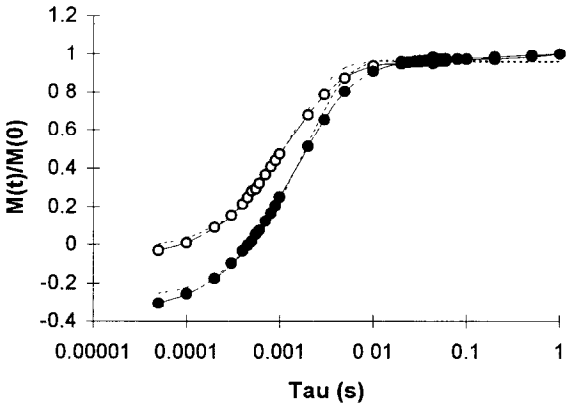

FIG. 5.

Stretch exponential least squares fit of equation 1 (i = 1, dotted line) and exponential least squares fit (β = 1, i = 2, solid line), to the decay data of sample S04 in virgin condition (○) and dried and resaturated condition (●).

Within experimental error (90% confidence interval) there is no observable changes in the relative volumes after drying and resaturation of the virgin samples. However, a notable and significant shift in the smaller spin-lattice relaxation times of samples S03 and S04 can be seen, suggesting that mainly the finer (micro and meso) portion of the pore system is affected by drying, corresponding to an opening of the structure (increase in the correlation time and thus increase in T_1). One should keep in mind, however, that the spin-lattice relaxation time of the confined pore water is more sensitive to changes in the pore size of smaller pores due to the approximate proportionality between $1/T_1$ and the inverse pore radius. This means that a corresponding change in pore dimension of the larger pores might be masked by the lack of sensitivity in T_1 for these larger pores.

Freeze/Thaw Cycling. The results from measurements of $T_{1,av}$ (single exponentials, $\beta = 1$) during freeze/thaw cycling of samples F04a,b,c and F06a,b,c are shown in Table 4. Within experimental uncertainty, no significant change in relaxation times could be observed between the start of the experiment (0 cycles) and after 5 cycles and 25 cycles, respectively. These results are in strong contrast to the actual physical condition of the samples as only one sample, S04c, was intact after 25 cycles. The other samples were completely fragmented. Most of the fragments measured were in the range of 0.5–3 mm. In light of the significant change observed in T_1 (and thus in the pore structure) during drying of these samples, it seems that the pore structure of cement pastes escapes virtually unharmed from exposure to the first 25 freeze/thaw cycles. This is consistent with the fact that water in very fine pores will freeze only at very low temperature. It does also support the idea of a largest critical distance (size of a sample) proposed by Fagerlund (30), below which freezing will not damage a porous structure. Thus, in the following discussion we have represented the three relaxation times corresponding to 0, 5 and 25 freeze/thaw cycles by their average value which is denoted by, $T_{1,initial}$. This relaxation time together with the relaxation time observed after 175 cycles are tabulated in Table 3. Also, the specific surface areas (S; derived using equation 4) are shown in Table 3. After 175 freeze/thaw cycles an increase in $T_{1,av}$ is observed,

TABLE 3

Spin lattice relaxation time, T_1, specific surface area (S), and relative volumes (in %) in cement pastes S03, S04, S06, S07a and S07b before and after drying at 105°C and resaturation with distilled water. T_1 is calculated by a non linear least squares fit to the magnetization decay curve using eq 1 with N = 2 and β = 1. Uncertainties are given as 90% confidence intervals

Sample	T_1 (ms)	S (m^2/g)	V (%)
S03, virgin	0.87 ± 0.12	162 ± 0.4	72 ± 4
	6.37 ± 2.26	8.6 ± 2.3	28 ± 4
S03, dried	2.35 ± 0.48	62.4 ± 10.6	75 ± 2
	8.99 ± 2.62	5.4 ± 1.23	25 ± 6
S04, virgin	0.81 ± 0 09	227 ± 22.4	65 ± 8
	3.22 ± 0.64	30.7 ± 5.1	35 ± 8
S04, dried	1.00 ± 0 10	175 ± 15.9	62 ± 6
	4.19 ± 0.65	25.6 ± 3.46	38 ± 6
S06, virgin	1.24 ± 0.10	306 ± 22.8	79 ± 3
	5.38 ± 1.03	18 8 ± 3.0	21 ± 3
S06, dried	1.24 ± 0.11	263 ± 21.5	68 ± 5
	4.51 ± 0.62	34.1 ± 4.1	32 ± 5
S07a, virgin	1.28 ± 0.16	239 ± 31.7	51 ± 5
	4 74 ± 0.67	62 ± 7 7	49 ± 5
S07a, dried	1.37 ± 0.25	223 ± 34.5	51 v 7
	4 73 ± 0.96	62.2 ± 3.4	49 ± 7
S07b, virgin	1.45 ± 0.18	253 ± 27.9	61 ± 5
	5.55 ± 1.11	42.2 ± 7.1	39 ± 5
S07b, dried	1.62 ± 0.22	245 ± 29.2	66 ± 5
	6.95 ± 1.77	29.4 ± 6 0	34 ± 5

corresponding to a reduction in specific surface area. With the exception of sample F06a, these changes are significant within a 90% confidence interval. As with the T_1 measurements, significant changes (reduction) in specific areas are seen after 175 freeze/thaw cycles. This indicates that the finer pore structure is affected after a sufficiently large number of freeze/thaw cycles. The amount of water present in the samples could be determined by integration of the water peak in the spectra. However, an increase in the water content in the specimens during the freeze/thaw cycling—which has been reported by others (10,31,32)—could not be verified as the samples deteriorated and made quantitative measurements difficult.

Conclusion

- The average T_1 in virgin hydrated cement pastes increases after drying at 105°C and resaturation with distilled water for all cement pastes investigated.
- Double exponential model fits to the observed NMR relaxation curves from virgin and

TABLE 4
T_1 and specific surface area (S) of sample series F04 and F06 during the start (0–25 cycles) and at the end (175 cycles) of a freeze/thaw experiment. Uncertainties are given as 90% confidence intervals

Sample	$T_{1,initial}$	$T_{1,175\ cycles}$	$S_{initial}$	$S_{175\ cycles}$
F04a	1.45 ± 0.01	1.91 ± 0.1	195 ± 3.4	163 ± 23
F04b	1.50 ± 0.01	1.77 ± 0.1	188 ± 3.5	157 ± 3.2
F04c	1.41 ± 0.01	1.65 ± 0.1	201 ± 3.6	166 ± 30.1
F06a	1.86 ± 0.01	1.90 ± 0.1	258 ± 3.8	263 ± 3.5
F06b	1.69 ± 0.03	1.91 ± 0.1	285 ± 3.8	261 ± 3.5
F06c	1.74 ± 0.01	2.01 ± 0.1	276 ± 3.8	253 ± 11.0

dried samples reveal a shift towards larger T_1 times of the confined water in the finer pores which is rationalized as a coarsening of the finer pore structure.

- ^1H spin lattice relaxation time T_1 in water occupying the pore system of hydrated cement pastes has been used to determine the specific surface area. The specific surface area is reduced by drying.
- NMR-line widths show significant decrease for w/c = 0.30, but line width measurements are less suited to study the drying process due to larger uncertainty and possibly different mechanisms governing the NMR line width and the T_1 relaxation rate.
- The results confirm earlier work indicating a coarsening of the pore structure as a result of drying.
- Significant changes in T_1 due to repeated freezing and thawing is only observed after 175 cycles. The effect is small and is consistent with the fact that water occupying micro and meso pores will freeze only at very low temperatures. The results are contrasted by the fact that five of six samples are fragmented by frost action already after 25 cycles, suggesting that the frost damage mechanism is more a macroscopic effect—due to pressure buildup—which is not affecting the micro and meso pores. It does also support the theory of a largest critical distance or size of a sample beyond which damage will occur while the pore system of the individual fragments is intact.

Acknowledgments

The work was financed by the Norwegian Research Council. The authors wish to thank Cand Scient Per Olav Kvernberg for kind assistance during the measurements.

References

1. T.C. Powers and T.L. Brownyard, Res. Labs. Portland Cement Association, Bulletin, 22 (March 1948).
2. H.C. Gran, M. Maage, T. Nilsen, K. Skjeggerud and E.J. Sellevold, Servicability of Concrete report No. 2—Frost durability, Report STF65 A86051, SINTEF, Trondheim, Norway, (in Norwegian), (1986).
3. T.C. Powers, L.E. Copeland, J.C. Hayes and H.M. Mann, ACI J., 285–298, (nov. 1954).

4. L.J. Parrot, W. Hansen and R.L. Berger, Cem. Concr. Res., 10, 647–655 (1980).
5. D.H. Bager and E.J Sellevold, Cem. Concr. Res., 16, 1–11 (1987).
6. E.J. Sellevold, Low temperature calorimetry as a pore structure probe, Proceedings 7th International Congress on the Chemistry of Cement, Vol. IV, Paris (1980).
7. C.D. Lawrence, The Interpretation of Nitrogen Sorption Isoterms on Hydrated Cement (Technical Report 530), Cement and Concrete Association, (1980).
8. D.N. Winslow and S.J. Diamond, Colloid and Interface Sci., 45, 425–426 (1973).
9. S. Jacobsen and E.J. Sellevold, Rapid freeze thaw testing of concrete—pore structure changes by cracking and healing. Concrete under severe conditions. K. Sakai, (ed.) pp 114–125, Chapman and Hall, New York (1995).
10. T.C. Powers, A working hypothesis for further studies of frost resistance of concrete, PCA-Bulletin No. 5 (1945).
11. A.R. Collins, in The Chemistry of Cement by F.M. Lea, 3rd edition, Edward Arnol Publishers Ltd., ISBN: 0 7131 2277 3, p. 611 (1983).
12. T.C. Powers and R.A. Helmuth, Proc. HRB, 32 (1953).
13. O.A. Kayyali, C.L. Page and A.G.B. Ritchie, ACI J., 1217–1225, Nov. (1976).
14. M. Nakamura, T. Fukushira and N. Kamitani, J. Ceram. Soc. Jpn., 100, 849–854 (1992).
15. H. Kukko, VTT Publication 126, Finland, (1992).
16. L.F. Gladden, Trans IChemE, Vol. 71, Part A, November (1993).
17. F. D'Orazio, J.C. Tarczon, W.P. Halperin, K. Eguchi and T. Mizusaki, J. Appl. Phys., 65, 742–751 (1989)
18. L.J. Schreiner, J.C. Mactavish, L. Miljkovi'c, M.M. Pintar, R Blinc, G. Lahajnar and L.W. Reeves, J. Am. Ceram Soc., 68, 10–16 (1985).
19. S. Bhattacharja, M Moukwa, F. D'Orazio, J-Y. Jehng and W.P. Halperin, Adv. Cem. Based Mater., 1, 67–76 (1993).
20. H.C Gran and E.W. Hansen, Submitted for publication (1996).
21 H.C. Gran and E.W. Hansen, Submitted for publication (1996).
22. R. Schmidt, E.W. Hansen, M. Stöcker, D. Akporiaye and O.H. Ellestad, J. Am. Chem. Soc., Vol. 117, (1995).
23. E.W. Hansen, R. Schmidt, M. Stöcker and D. Akporiaye, J. Phys. Chem., 99, 4148–4154 (1995).
24. D.P. Gallegos, K. Munn, D.M. Smith and D. Stermer, J. Colloid Interface Sci., 119, 127–140 (1987).
25. M.H. Cohen and K S. Mendelson, J. Applied Phys., 53, 1127–1135 (1982).
26. L. Barbic, I. Kocuvan, R. Blinc, G. Lahajnar, P. Merljak and I. Zupancic, 7th International Congress on the Chemistry of Cement, Paris, pp. 25–31 (1980).
27. M. Letellier, H. Van Damme, B. Mortureux and M. Regourd, in 8th International Conference on Chemistry of Cement, Vol. 3, pp. 93–100, (1986)
28. J.R. Zimmermann and W.E Brittin, J Phys. Chem., 61, 1328–1333 (1957).
29. N. Bloembergen, E.M. Purcell and R.V. Pound, Phys. Rev., 73, 679 (1948).
30. G. Fagerlund, Studies of the destruction mechanism at freezing of porous materials, 6th International Congress on Problems Raised By Frost Action, Le Havre (1975).
31. G. Fagerlund, Nordic Concr. Res., 11, 20–36 (1992).
32. V. Hartmann, Optimizing and Calibration of frost/salt scaling testing of concrete CDF-test. Dr. Ing. Dissertation Universität—GH—Essen (in German) (1993).